Journal of Renewable Materials

Tech Science Press

DOI: 10.32604/jrm.2023.025271

check for updates

ARTICLE

Ammonium Metavanadate Fabricated by Selective Precipitation of Impurity Chemicals on Inorganic Flocculants

Bo Shi[1], Dandan Zhu[2,*], Pengxiang Lei[3], Ximin Li[4], Hengbo Xiao[4] and Lihua Qian[4,*]

[1]Shandong Aluminum Industry Corporation Limited, Zibo, China

[2]Petroleam & Natural Gas Transport Corporation of China, Wuhan, China

[3]School of Chemistry and Chemical Engineering, Hubei University of Technology, Wuhan, China

[4]School of Physics, Huazhong University of Science and Technology, Wuhan, China

[*]Corresponding Authors: Dandan Zhu. Email: zhudandan123@cnpc.com.cn; Lihua Qian. Email: lhqian@hust.edu.cn

Received: 02 July 2022 Accepted: 04 August 2022

ABSTRACT

High purity ammonium metavanadate (NH_4VO_3) is the most vital chemical to produce V_2O_5, VO_2, VN alloy, VFe alloy and $VOSO_4$, which have some prospective applications for high strength steel, smart window, infrared detector and imaging, large scale energy storage system. NH_4VO_3 is usually produced by spontaneous crystallization from the aqueous solution due to its sharp dependence of solubility on the temperature. However, hazardous chemicals in industrial effluent, include phosphorate, silicate and arsenate, causing severe damage to the environment. In this work, these impurities are selectively precipitated onto inorganic flocculants, while the vanadate dissolved in an aqueous solution keeps almost undisturbed. Therefore, high purity NH_4VO_3 is produced by the crystallization from the purified solution. By screening various flocculants and precipitating parameters, polyaluminum sulfate with an optimal amount of 50 g/L, is demonstrated to selectively remove phosphorate, silicate and arsenate, corresponding to the removing efficiency of 93.39%, 97.11% and 88.31%, respectively. NH_4VO_3 from the purified solution holds a purity of 99.21%, in comparison with 98.33% in the product from the crude solution. This purifying technology cannot only produce NH_4VO_3 with high added value, but also reduce the environmental pollution of waste liquid.

KEYWORDS

Ammonium metavanadate; flocculating agent; phosphate; arsenate; cooling precipitation; vanadium slag; bayer alumina liquor

1 Introduction

Ammonium metavanadate (NH_4VO_3) and its derivatives are scarce resources in iron and steel metallurgy [1], aerospace industry [2], information technology [3], sustainable energy [4,5], artificial intelligence [6] and smart window [7–12]. Vanadium alloys are important additives in precipitating strengthened steel, where dispersive nanoparticles with ultrahigh strength become the obstacle to dislocation motion [13]. Metal-insulator phase transition of VO_2 enables modulating the reflection of infrared light while keeping stable transparency in visible regions [14–16]. This phase transition depends on the types of metallic cations and their doping levels, showing attractive applications in self-protective

optical devices [17,18] and smart windows. The vanadium flow battery is a prospective system that can serve for long-term and large-scale storage of sustainable energy [19,20]. These prospective applications greatly depend on the purity of NH_4VO_3, a vital precursor to produce the intermediate V_2O_5 and VO_2 for infrared devices, V.N., and VFe alloys for high-strength steel, and $VOSO_4$ for vanadium electrolyte in the flow battery.

The solubility of NH_4VO_3 in an aqueous solution has steep dependence on the temperature compared with the other salts. This specific feature is a fundamental principle for precipitating NH_4VO_3 powder by means of crystallization during the cooling process. Unfortunately, simultaneous precipitations of phosphate, silicate, arsenate and other impurity elements are inevitable. These impurities are usually found in many solid slags containing vanadium, which significantly depends on raw resources and makes a dominant contribution to the quantity of NH_4VO_3 crystal. For Bayer alumina smelting, a mature technique enabled the effective extraction of solid slag several years ago [21]. This slag includes sodium oxalate, sodium carbonate, sodium phosphate, sodium silicate, sodium arsenate and sodium vanadate. The mass fraction of sodium vanadate in this slag can reach 11%~18% amazingly, which is good raw material to produce NH_4VO_3. All the chemicals in the slag are dissolved into the water as a crude solution containing vanadate anions which should be initially purified by removing some other water-soluble salts. However, various water-soluble impurities in the waste liquid are produced after impurity removals, such as phosphate and arsenate anions. If these polluting impurities are discharged into the natural environment, they will seriously damage the water quality and accumulate in the soil. Subsequent assimilation of crops and animals further causes serious harm to society and the environment. Therefore, the separation of these polluting qualifications in the process of impurity removal not only improves the purity of ammonium metavanadate but also reduces environmental pollution and promotes environmental protection.

To avoid simultaneous precipitation of several impurities during the crystallization of NH_4VO_3, the unexpected impurity in aqueous mixtures must be removed in advance. General methods to remove impurities from crude solutions include chemical precipitation, ion exchange, solvent extraction, membrane separation, etc. Amongst these methods, chemical precipitation is a suitable way to remove low concentration impurities from crude solutions because of its simple equipment and high processing capacity. Some previous investigations have tried flocculants as chemical precipitants to remove impurities [22]. However, the unsolved problem of chemical precipitation is that many flocculants cannot selectively remove impurities while minimizing the loss of target elements. Therefore, finding suitable flocculant and optimizing specific crystallization conditions are significantly important.

Herein, we developed one practical way to improve the purity of NH_4VO_3 via selective precipitation and filtration of impurity salts. Systematical experiments aim to investigate the chemical precipitation of some relative salts on various flocculants. Polyaluminum sulfate (PAS) is experimentally demonstrated to be a candidate to remove impurity salts effectively. Keeping the negligible loss of vanadate in the same condition makes it a reality to fabricate high purity NH_4VO_3 by subsequent crystallization. In our investigation, PAS can remove the polluting arsenate and phosphate while retaining vanadium anions in the solution. Thus, it has a good perspective for the selective recovery of the vanadium element. On one hand, extractions of phosphate and arsenate can avoid soil and underground water pollution after direct drainage. On the other hand, PAS can retain vanadium in solution, providing an effective technique for subsequent production of NH_4VO_3 with high added value.

2 Experimental Procedures

2.1 Materials and Chemicals

Solid slag consisting of various salts used in this experiment is extracted by Bayer alumina process in China Aluminum Shandong Co., Ltd. (China). Polyaluminum sulfate (PAS), polyaluminum chloride (PAC),

polyferric sulfate (PFS), magnesium sulfate ($MgSO_4$), and calcium oxide (CaO) as industrial products were provided by Zibo Zhenghe Water Purification Co., Ltd. (China). Chemical Reagents, including sulfuric acid, ammonium sulfate, magnesium sulfate, and calcium oxide, were purchased from China National Medicines Co., Ltd. (China). These reagents were analytical grade and used without further purification.

2.2 Chemical Precipitation

Some salts can react with inorganic flocculants with a precipitated production that is water insoluble. Chemical precipitation is widely used for water purification and treatment. In our experiment, the impurities, including phosphate, arsenate, and silicate anions, were highly water soluble. After chemical adsorption onto the PAS, subsequent precipitation of aluminum phosphate, aluminum arsenate, and aluminum silicate were separated from the crude solution, with a subsequent formation of a purified solution.

2.3 NH_4VO_3 Crystallization

The purified solution with a volume of 500 ml was heated to 50°C. 60 g ammonium sulfate was added into the solution with a continuous stirring for 60 min. The pH value is adjusted to 8–9 by introducing a diluted H_2SO_4 solution. When this solution is cooled to room temperature naturally, spontaneous crystallization of NH_4VO_3 powder occurred. The powders were filtered by industrial gauze, washed with water, and dried in the air.

2.4 Microstructural Characterization

The phases of chemical products were analyzed by X-ray diffractometer (Bruker D2 type X-ray diffractometer). The Cu-Kα radiation (λ = 1.54060) was produced under an accelerating voltage of 30 kV and a current of 10 mA. 2θ acquisition in a range of 10°∼80° is carried out with a step is 0.017°/s. Raman spectroscopy at a range of 100∼4000 cm^{-1} was conducted in a Raman microscope (Ramos S120, Ostec-ArtTool, LLC, Moscow) equipped with an objective with a working distance of 8 mm. The wavelength of the exciting laser was 532 nm. X-ray photoelectron spectroscopy (XPS) was performed on an AXIS-ULTRA DLD-600W spectrometer with monochromatic Al K_α (1486.71 eV). The optical properties of spherical KBr were studied by Fourier transform infrared spectrometer (FTIR, Nicolet iS50R). Inductively coupled plasma mass spectrometry (ICP-OES, Thermo fisher iCAP7200) was carried out to measure the concentration of various elements.

2.5 Precipitation Capacity

The removal of P, Si, and As from crude solution by PAS was studied. The following parameters were studied by batch adsorption of three kinds of anions containing these impurities (P, Si, As): adsorption capacity and kinetics [23]. In all the adsorption experiments, 5 g PAS was added to 100 mL crude solution, stirred at 60°C, and then filtered to obtain the purified solution. The concentration of impurity elements in this purified solution was tested by ICP. The adsorption capacity (Q_e, mg/g) of PAS for P, Si and As was estimated by the equation.

$$Q_e = \frac{(C_0 - C_t)V_0}{W} \tag{1}$$

where Q is the adsorption capacity (mg/g), C_0 and C_t are the initial concentration and the concentration of silicon/phosphorus/arsenic in solution (mg/L) at time t. V_0 is solution volume, and W is the weight of PAS (g).

3 Results and Discussions

The compositions of solid slag extracted from the mother liquid during Bayer alumina smelting are listed in Table 1. Mass fraction of V_2O_5 (V_2O_5 is utilized to calibrate the quantity of sodium metavanadate. Other elements are calibrated in the same case) occupies 14.95%. Mass fraction of Al_2O_3, P_2O_5, SiO_2 and As_2O_3

respectively occupy 2.75%, 3.48%, 0.39% and 3.85%. Residual mass is organic materials, including humic acid and oxalate. In our experiments, solid slag is dissolved into water as a crude solution, which can be purified by several flocculants, enabling the removal of P_2O_5, SiO_2, and As_2O_3. The flocculants used here include aluminum sulfate ($Al_2(SO_4)_3$), polyaluminum sulfate (PAS), polyaluminum chloride (PAC), polymerized ferric sulfate (PFS), magnesium sulfate ($MgSO_4$), calcium oxide (CaO), etc. The intermediate solution that contains the dissolved slag and certain flocculants is continuously stirred at 30°C for 60 min. Pressure filtration will create the purified solution with instantaneous solidification of the wastes that consist of the impurities precipitated on flocculants. ICP-OES evaluates the quantitative contents of the relevant chemicals in the purified solution.

Table 1: Mass fraction of different chemicals in solid slag from bayer alumina smelting. The concentrations of different contents are weighed by their corresponding compounds

Contents (mass%)	V_2O_5	Na_2O	Al_2O_3	P_2O_5	SiO_2	As_2O_3	Organic	Residual
Solid slag	14.95	50.97	5.05	6.39	0.72	7.06	13.55	1.31

To evaluate the removal efficiency of impurities on the above flocculants, mass fractions of vanadate, phosphorate, silicate, and arsenate in the purified solution are quantitatively measured compared with the crude solution. The detailed procedure from solid slag to NH_4VO_3 is schematically illustrated in Fig. 1.

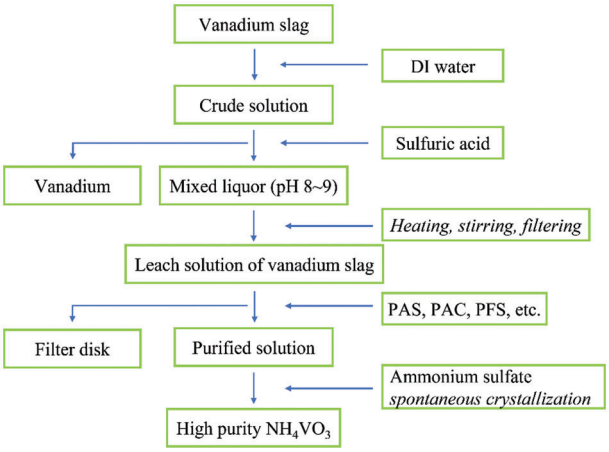

Figure 1: Schematic illustration to remove the impurity in solid slag and produce high purity NH_4VO_3. The processing routes are emphasized in italics

Quantitative analysis in Fig. 2a indicates that only 1.8% loss of vanadium in PAS is 1/6 and 1/5 compared to the losses in CaO and PFS, respectively. It is demonstrated that PAS possesses the weakest adsorption of vanadium. Meanwhile, more than 45% of phosphorate is removed as shown in Fig. 2b, while adsorptive capacity is almost three times better than that of $MgSO_4$. This manifests that the phosphorate can be effectively precipitated onto PAS.

In addition, PAS also holds the best ability to remove silicate and arsenate with mass reductions of 62% and 36%, as illustrated in Figs. 2c and 2d, respectively. Based on the above quantitative analysis, PAS leads to a negligible loss of vanadium and highly efficient precipitation of impurities such as phosphorate, silicate,

and arsenate, which demonstrate that PAS can be regarded as a potential candidate to remove the impurity salts effectively and maintain the content of vanadate at the same time.

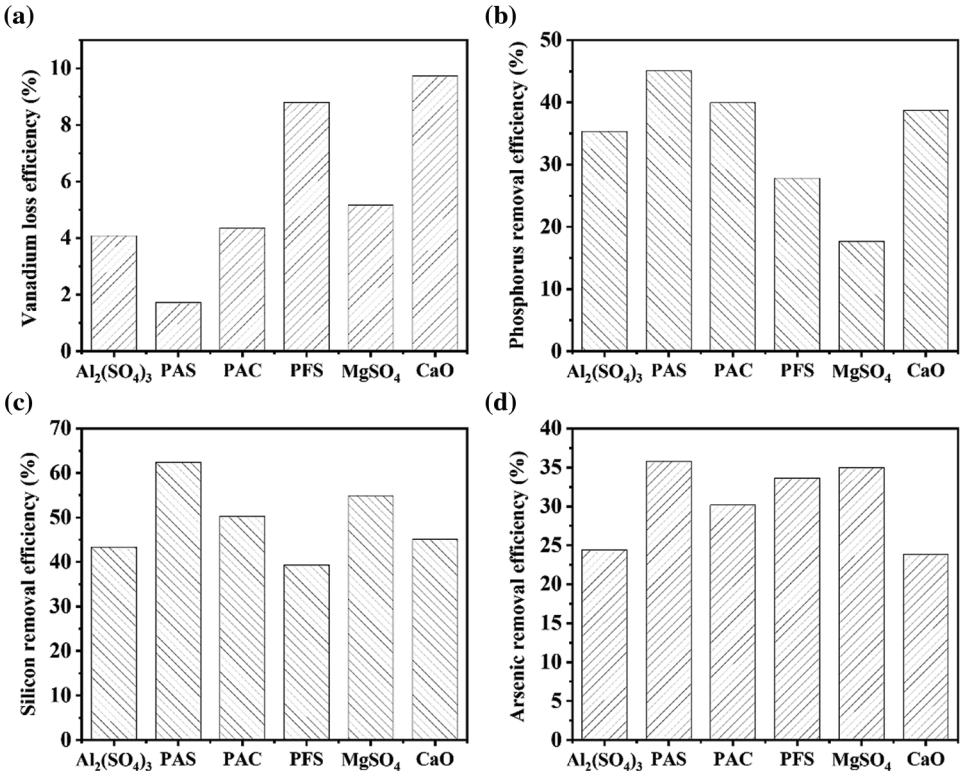

Figure 2: The loss percentages of different impurities corresponding to (a) vanadium, (b) phosphorus, (c) silicon, and (d) arsenic elements are estimated in the purified solution, which is treated by several inorganic flocculants

After considering the purifying efficiency of various flocculants, the PAS can be selected to determine the detailed flocculation parameters, e.g., the dosage of flocculants, solution temperature, and precipitating time. Firstly, PAS powders with different dosages are added into a 100 mL crude solution where 50 g solid slags are initially dissolved. This intermediate solution is stirred for 60 min at 30°C, and obtain the purified solution after pressure filtration. By comparing with the concentration of impurities in crude and purified solution illustrated in Fig. 3a, we can observe that the removal efficiency of P that is directly proportional to the dosage of PAS reaches ~90% when less than 5 g is supplied. However, the removal efficiency reaches saturation after a further dose toward 7 g.

Interestingly, a similar tendency can be obtained for the purification of Si and As elements, whose saturation efficiencies can reach 92% and 80%, respectively. Unlike a significant decrease of P, Si, and As concentration, the loss of vanadium element can be neglected in the same case, only less than 10% in the case of 7 g PAS addition. Besides the effect of flocculant dosage, the saturation efficiency in removing P, Si, and As also depends on solution temperature, as shown in Fig. 3b. Their saturation values at 60°C reach the summits corresponding to 92%, 97%, and 86%, respectively. In comparison, the removal efficiency for vanadium behaves in completely different ways, showing a nearly constant of 5%. Finally, the precipitating kinetic of impurities on the PAS is also investigated by changing the precipitating time as shown in Fig. 3c. The removing efficiency of different elements lifts quickly in the

initial 30 min, with a subsequent saturation of 90% for P, Si and As. In the same condition, removing efficiency for vanadium elements is below 4%, which indicates that PAS can effectively precipitate impurity chemicals such as phosphorate, silicate, and arsenate in a short duration. The loss of vanadium content is almost negligible.

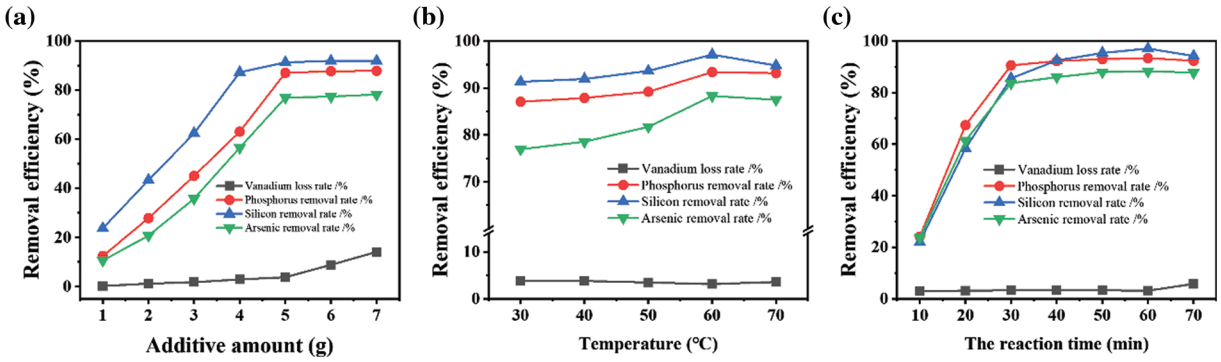

Figure 3: The purification efficiency of PAS is represented based on several experimental parameters: (a) the dosage of flocculants, (b) the operating temperature, and (c) precipitating time

Based on the dependence of purifying capability on these parameters, one potential application is to generate high purity NH_4VO_3 by cooling crystallization. Various techniques are utilized to characterize the detailed microstructures and composition of correlated materials to clarify the purifying mechanism. Firstly, two kinds of NH_4VO_3 powders are produced by cooling precipitation of crude (c-NH_4VO_3) and purified (p-NH_4VO_3) solution. The ICP-OES was carried out on NH_4VO_3 to measure the concentration of impurity elements, as shown in Fig. 4a. The contents of Si, P, and As in c-NH_4VO_3 are 0.056%, 0.12%, and 0.092%, respectively. By contrast, the contents of Si, P, and As in p-NH_4VO_3 sharply reduce to 0.041%, 0.018%, and 0.033%, respectively. Notably, the content of phosphorus in p-NH_4VO_3 decreases by approximately 85.2% in comparison with that in c-NH_4VO_3. Lower removing efficiency corresponding to 26.8% and 64.1% are obtained for Si and As elements. It is obvious that the concentration of p-NH_4VO_3 is as much as 99.2%, which is much higher than that of c-NH_4VO_3 (98.33). Besides ICP characterization, the XPS is utilized to evaluate the valence state of the P element, as shown in Fig. 4b. Peak at 134.13 eV is attributed to the P^{3+} 2p peak [24]. It is noteworthy that nearly no P 2p signal is detected in p-NH_4VO_3. It indicates that most PO_4^{3-} ions are removed by PAS, behaving coherently results in the ICP.

In comparison with P elements, XPS of Si and As elements are detected in both c-NH_4VO_3 and p-NH_4VO_3 powders, as shown in Figs. 4c and 4d, implying partial purification of silicate and arsenate in crude solution. Besides, the XPS is also carried out on the disk obtained by pressure filtration of the purified solution, as shown in Figs. 5a–5c. It can be seen that the obvious signal of As 3d peak and P 2p peak, together with a weak signal of the Si 2p peak [25–28].

Raman spectroscopy also enables characterizing the microstructures and impurity in c-NH_4VO_3 and p-NH_4VO_3 powders in Fig. 4e. Obviously, all sharp bands correspond to various vibrations of atomic bonding in NH_4VO_3. Raman spectra in c-NH_4VO_3 and p-NH_4VO_3 powders exhibit a noticeable difference in the background. The background in p-NH_4VO_3 can be negligible, demonstrating valid precipitation of impurity on PAS. Broad background covering from 1200–3000 cm^{-1} is visible in the c-NH_4VO_3, implying strong fluorescence of some impurities embedded in the c-NH_4VO_3. To clarify the mechanism of the fluorescence background, Raman spectra of phosphate and silicate are also collected. The Raman spectrum of $AlPO_4$ in Fig. 4f exhibits strong fluorescence, which seriously surpasses the

intrinsic Raman scattering of PO_4^{3-}anions. The fluorescence background represents the nearly identical feature between $AlPO_4$ and c-NH_4VO_3, demonstrating that PO_4^{3-} ions are the dominant impurity in c-NH_4VO_3. In addition, Raman spectra of NaH_2PO_4 and K_2HPO_4 also show a visibly broad peak in the range of 1200–3000 cm^{-1}, which further confirms that the fluorescence background is caused by phosphate as shown in Figs. 6a–6c. Based on the above analysis, we hold that PAS can significantly reduce the concentration of PO_4^{3-} in crude solution, which effectively improves the purity and quality of NH_4VO_3.

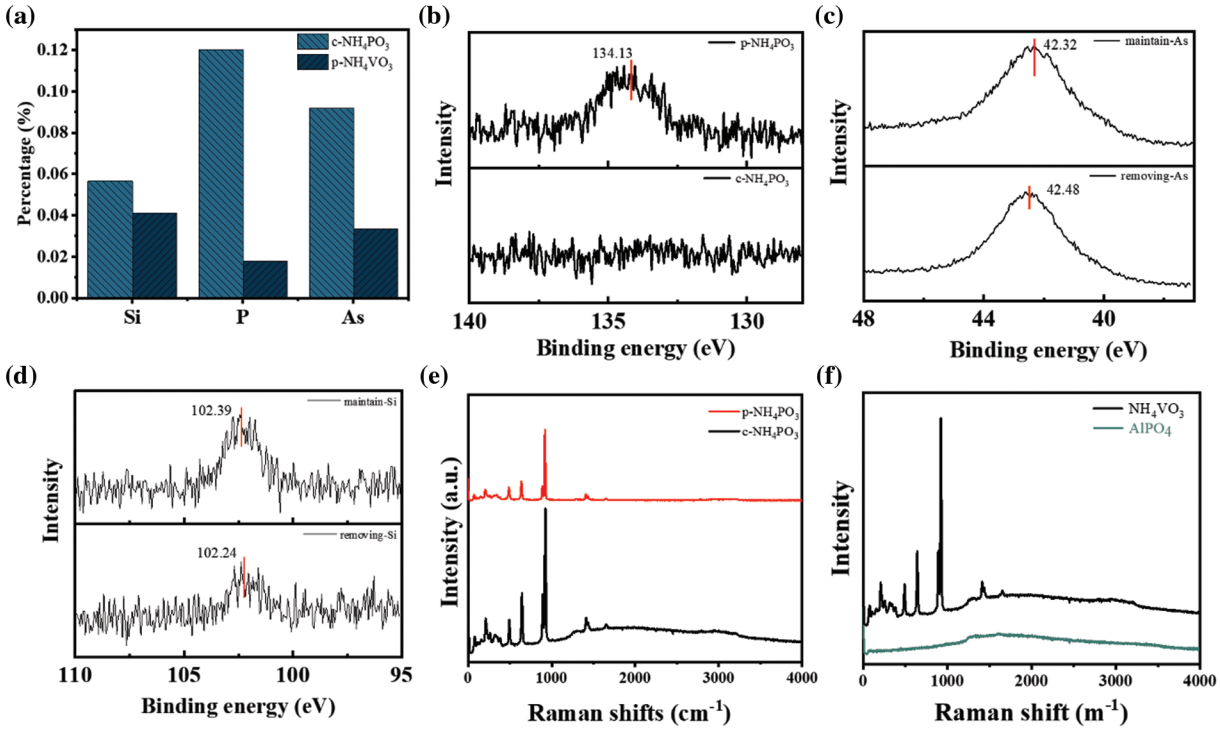

Figure 4: (a) The contents of Si, P, and As in c-NH_4VO_3 and p-NH_4VO_3; XPS spectra and their deconvolutions of c-NH_4VO_3 and p-NH_4VO_3 corresponding to (b) P 2p peak, (c) As 3d peak and (d) Si 2p peak; (e) Raman spectra of c-NH_4VO_3 and p-NH_4VO_3; (f) Raman spectra of NH_4VO_3 and $AlPO_4$

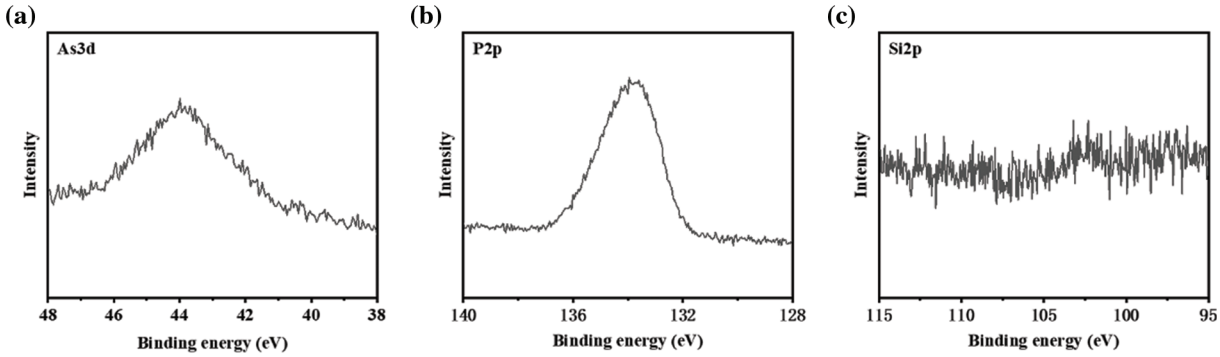

Figure 5: XPS spectra and their deconvolutions of the disk from filtered disk corresponding to (a) As 3d peak, (b) P 2p peak, and (c) Si 2p peak

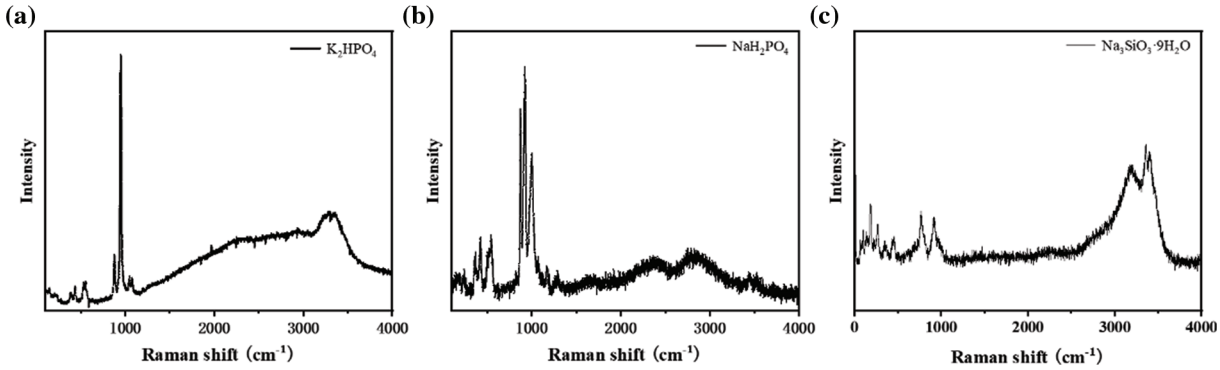

Figure 6: Raman spectra of (a) K_2HPO_4, (b) NaH_2PO_4 and (c) Na_2SiO_3

Based on the negligible XPS signals of the P element in p-NH_4VO_3, it can be concluded that most PO_4^{3-} anions in crude solution are precipitated on PAS selectively. Precipitations of some impurities are intrinsically physical and chemical adsorptions on the PAS. Many quantitative models are developed to describe an intrinsic mechanism of adsorption kinetics [29–31]. First-order, second-order and intraparticle diffusion models are normally described as Eqs. (2)–(4):

$$\ln(Q_e - Q_t) = \ln Q_e - k_1 t \tag{2}$$

$$\frac{t}{Q_t} = \frac{1}{k_2 Q_e^2} + \frac{t}{Q_e} \tag{3}$$

$$Q_t = k_{in} t^{1/2} + const \tag{4}$$

where Q_e (mg/g) and Q_t (mg/g) are adsorption quantities of P, Si, and As elements at equilibrium time t (min), respectively. k is the rate constant of three different adsorption mechanisms. Based on linear relations from these three models, experimental data is fitted in Fig. 7. The second-order model looks more suitable to describe the adsorption kinetics of P, Si and As onto the PAS. Their fitting parameters tabulated in Table 2 correspond to 0.9789, 0.9463, and 0.9771, respectively. Good fitting based on the second-order model indicates the chemical adsorption of silicate, phosphate and arsenate onto the PAS.

When many kinds of anions exist in crude solution, removing these anions at room temperature is considered to operate via chemical adsorption. This mechanism is verified by chemical adsorptions of some anions containing V, Ga elements onto the flocculants [23,30,32,33]. In our investigation, we believe this mechanism also works during the chemical adsorptions of silicate, phosphate and arsenate onto the PAS. Good fitting based on the second-order adsorption model also supports this mechanism.

As we all know, the Bayer process is widely applied in industrial alumina production. Currently, effective recoveries of hazard elements and valuable elements become the key issue for environmental protection and comprehensive utilization of mineral resources. From the viewpoint of an environmental aspect, the developed flocculants in our work not only benefit vanadate recovery with the production of ammonium metavanadate with high purity, but also concentrate arsenates and phosphates into the flocculants that are harmful to underground water and soils. From viewpoint of the economic aspect, the extracted vanadium from Bayer liquid in industrial alumina factories can create additional profits. Meanwhile, removing the vanadium element from Bayer liquid will reduce the impurities in alumina particles, improving the quantities of their derivative products, such as pure aluminum and aluminum alloys. In general, chemical precipitation of impurity on flocculants helps the vanadium recovery and avoids environmental destruction after direct drainage of wastewater containing hazardous elements.

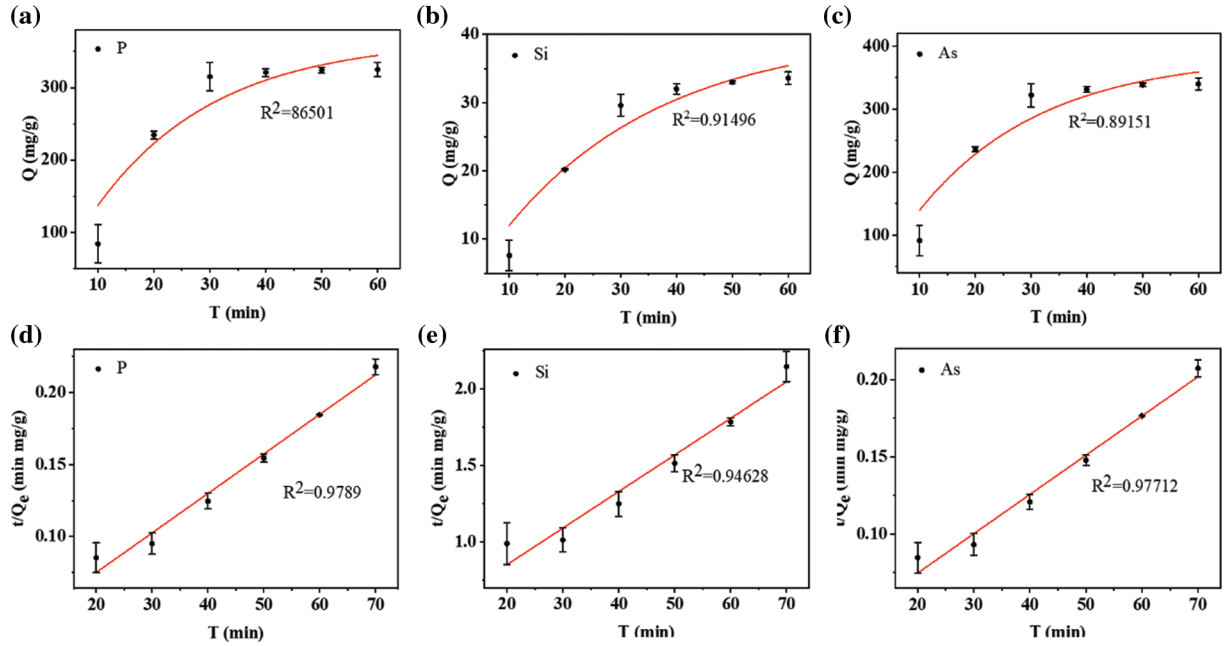

Figure 7: Pseudo-first-order kinetic plots for the adsorption of (a) P, (b) Si, and (c) As; Pseudo-second-order kinetic plots for the adsorption of (d) P, (e) Si, and (f) As

Table 2: Kinetic parameters fitted from first-order, second-order kinetic, and intra-particle diffusion models

Kinetics model	Parameters	P	Si	As
	k_1	0.071	0.0519	0.0651
First-order	Q_e	333.024	36.111	350.498
	R^2	0.812	0.8627	0.8549
	k_2	3.73E − 4	0.00153	2.70E − 4
Second-order	Q_e	364.364	41.829	393.458
	R^2	0.9789	0.94628	0.97712
	k_{in}	18.567	2.939	22.419
Intra-particle diffusion	I	184.662	10.841	170.203
	R^2	0.465	0.632	0.558

4 Conclusions

In summary, we investigate the purification of crude solutions containing vanadium by utilizing impurity precipitation on various flocculants. PAS is the most effective flocculant to remove P, Si, and As elements, while keeping the negligible loss of vanadium element. The purifying ability is optimized from some parameters when the precipitating time of 60 min, when the operating temperature of 60°C and the dosage of PAS of 50 g/L are applied. In these conditions, the removal efficiency of phosphorus, silicon, and arsenic is 93.4%, 97.1%, and 88.3%, respectively, while the vanadium loss efficiency of 3.1% is the lowest. High purity NH_4VO_3 with a content of 99.2% is obtained from the purified solution. After the detailed characterization, some PO_4^{3-} anions in the NH_4VO_3, which are crystallized from the purified solution, show a negligible fluorescence background in the Raman spectrum. By fitting experimental data

based on three adsorption kinetics models, pseudo-second-order kinetics is proposed to make the dominant contribution to the impurity precipitation.

Funding Statement: We acknowledge financial support from the Natural Science Foundation of Hubei Province (2020BED011). XPS characterizations and ICP-OES were carried out in the Analytical and Testing Center in HUST.

Conflicts of Interest: The authors declare they have no conflicts of interest to report regarding the present study.

References

1. Qiu, W., Liu, Z., Yu, R., Chen, J., Ren, Y. H. et al. (2019). Utilization of VN particles for grain refinement and mechanical properties of AZ31 magnesium alloy. *Journal of Alloys & Compounds, 781,* 1150–1158. DOI 10.1016/j.jallcom.2018.12.124.
2. Hovsepian, P. E., Luo, Q., Robinson, G., Pittman, M., Howarth, M. D. et al. (2006). Tialn/vn superlattice structured pvd coatings: A new alternative in machining of aluminium alloys for aerospace and automotive components. *Surface and Coatings Technology, 201(1–2),* 265–272. DOI 10.1016/j.surfcoat.2005.11.106.
3. Ge, L., Yuan, N., Li, J., Chen, X. (2006). Thermal simulation of micromachined bridge and self-heating for uncooled VO_2 infrared microbolometer. *Sensors & Actuators A Physical, 126(2),* 430–435. DOI 10.1016/j.sna.2005.10.041.
4. Lee, C. Y., Jiang, C. A., Hsieh, C. L., Chen, C. H., Huang, Y. P. (2017). Application of flexible integrated microsensor to internal real-time measurement of vanadium redox flow battery. *Sensors and Actuators A Physical, 267*. DOI 10.1016/j.sna.2017.10.011.
5. Shao, Y., Wang, X., Engelhard, M., Wang, C., Sheng, D. L. et al. (2016). Nitrogen-doped mesoporous carbon for energy storage in vanadium redox flow batteries. *Journal of Power Sources, 195(13),* 4375–4379. DOI 10.1016/j.jpowsour.2010.01.015.
6. Kumar, M., Park, J. Y., Seo, H. (2021). An artificial mechano-nociceptor with mott transition. *Small Methods, 5,* 2100566. DOI 10.1002/smtd.202100566.
7. Zhang, C., Gao, Y., Kang, L., Jing, D., Zhang, Z. L. et al. (2011). VO_2-based double-layered films for smart windows: Optical design, all-solution preparation and improved properties. *Solar Energy Materials & Solar Cells, 95(9),* 2677–2684. DOI 10.1016/j.solmat.2011.05.041.
8. Zhao, Y., Xu, R., Zhang, X., Hu, X., Knize, R. J. L. et al. (2013). Simulation of smart windows in the ZnO/VO_2/ZnS sandwiched structure with improved thermochromic properties. *Energy and Buildings, 66,* 545–552. DOI 10.1016/j.enbuild.2013.07.071.
9. Kim, J., Ejiri, T., Sugiyama, M. (2020). Investigation of VO_2 directly deposited on a glass substrate using rf sputtering for a smart window. *Japanese Journal of Applied Physics, 59(10),* 105506. DOI 10.35848/1347-4065/abbb1d.
10. Shen, N., Chen, S., Shi, R., Niu, S., Cheng, C. (2021). Phase transition hysteresis of tungsten doped VO_2 synergistically boosts the function of smart windows in ambient conditions. *ACS Applied Electronic Materials*. DOI 10.1021/acsaelm.1c00550.
11. Shi, C., Wang, Z., Hui, R., Chen, Y., Zou, C. (2019). Gate-controlled VO_2 phase transition for high-performance smart windows. *Science Advances, 5(3),* eaav6815. DOI 10.1126/sciadv.aav6815.
12. Chang, T., Cao, X., Li, N., Long, S., Gao, X. D. et al. (2017). Facile and low-temperature fabrication of thermochromic CR_2O_3/VO_2 smart coatings: Enhanced solar modulation ability, high luminous transmittance and UV-shielding function. *Chromium Compounds, 9(31),* 26029–26037. DOI 10.1021/acsami.7b07137.
13. Chen, W., Shi, Z., Zhao, Y. (2010). Research of HRB500E high-strength earthquake-proof bars produced by V.N. alloy and MnSiN12 process. *Hot Working Technology.* DOI 10.3788/HPLPB20102208.1780.
14. Lu, H., Clark, S., Guo, Y., Robertson, J. (2021). The metal–insulator phase change in vanadium dioxide and its applications. *Journal of Applied Physics, 129(24),* 240902. DOI 10.1063/5.0027674.

15. Jian, Z., Chen, X., Lei, X. (2018). Phase transition performance recovery of w-doped VO_2 by annealing treatment. *Materials Research Express, 5(6)*. DOI 10.1088/2053-1591/aacd8c.
16. Li, K., Li, M., Xu, C., Luo, Y., Li, G. (2019). VO_2(M) nanoparticles with controllable phase transition and high nanothermochromic performance. *Journal of Alloys and Compounds, 816,* 152655. DOI 10.1016/j.jallcom.2019.152655.
17. Wang, Y. Q., Gang, Y., Huang, Z. J., Ying, H. (2016). Infrared laser protection of multi-wavelength with high optical switching efficiency VO_2 film. *Acta Physica Sinica, 65(5),* 057102. DOI 10.7498/aps.65.057102.
18. Chen, X. R., Hu, J. Z., Han, W. Z. (2007). Study on pulse laser damage of vanadium oxide thin film. *Transactions of Materials and Heat Treatment, 28(4),* 373–374. DOI 10.13067/JKIECS.2014.9.2.195.
19. Li, X., Zhang, H., Mai, Z., Zhang, H., Vankelecom, I. (2011). Ion exchange membranes for vanadium redox flow battery (VRB) applications. *Energy & Environmental Science, 4(4),* 1147–1160. DOI 10.1039/c0ee00770f.
20. Kear, G., Shah, A. A., Walsh, F. C. (2012). Development of the all-vanadium redox flow battery for energy storage: A review of technological, financial and policy aspects. *International Journal of Energy Research, 36(11)*. DOI 10.1002/er.1863.
21. Li, Y., Zeng, X., Liu, Y., Yan, S., Ni, Y. (2003). Study on the treatment of copper-electroplating wastewater by chemical trapping and flocculation. *Separation & Purification Technology, 31(1),* 91–95. DOI 10.1016/S1383-5866(02)00162-4.
22. Hind, A. R., Bhargava, S. K., Grocott, S. C. (1999). The surface chemistry of bayer process solids: A review. *Colloids & Surfaces A: Physicochemical & Engineering Aspects, 146(1–3),* 359–374. DOI 10.1016/S0927-7757(98)00798-5.
23. Zhao, Z., Li, X. H., Chai, Y. Q., Hua, Z. S., Xiao, Y. P. et al. (2015). Adsorption performances and mechanisms of amidoxime resin toward gallium(III) and vanadium(V) from Bayer liquor. *ACS Sustainable Chemistry & Engineering, 4(1)*. DOI 10.1021/acssuschemeng.5b00307.
24. Khattak, G., Mekki, A., Gondal, M. (2013). XPS studies of pulsed laser induced surface modification of vanadium phosphate glass samples. *Journal of Physics and Chemistry of Solids, 74(1),* 13–17. DOI 10.1016/j.jpcs.2012.07.010.
25. Lim, S. F., Zheng, Y. M., Zou, S. W., Chen, J. P. (2009). Uptake of arsenate by an alginate-encapsulated magnetic sorbent: Process performance and characterization of adsorption chemistry. *Journal of Colloid & Interface Science, 333(1),* 33–39. DOI 10.1016/j.jcis.2009.01.009.
26. Lim, S. F., Zheng, Y. M., Chen, J. P. (2009). Organic arsenic adsorption onto a magnetic sorbent. *Langmuir, 25(9),* 4973–4978. DOI 10.1021/la802974x.
27. Liu, A., Wang, W., Liu, J., Fu, R., Zhang, W. X. (2018). Nanoencapsulation of arsenate with nanoscale zero-valent iron (nZVI): A 3D perspective. *Science Bulletin, 63(24),* 1641–1648. DOI 10.1016/j.scib.2018.12.002.
28. Dalby, K. N., Nesbitt, H. W., Zakaznova-Herzog, V. P., King, P. L. (2007). Resolution of bridging oxygen signals from O 1s spectra of silicate glasses using XPS: Implications for O and Si speciation. *Geochimica et Cosmochimica Acta, 71(17),* 4297–4313. DOI 10.1016/j.gca.2007.07.005.
29. Zhao, Z., Cui, L., Guo, Y., Gao, J., Li, H. et al. (2021). A stepwise separation process for selective recovery of gallium from hydrochloric acid leach liquor of coal fly ash. *Separation and Purification Technology, 265,* 118455. DOI 10.1016/j.seppur.2021.118455.
30. Du, J., Zhang, M., Dong, Z., Yang, X., Zhao, L. (2022). Facile fabrication of tannic acid functionalized microcrystalline cellulose for selective recovery of Ga(iii) and In(iii) from potential leaching solution. *Separation and Purification Technology, 286,* 120442. DOI 10.1016/j.seppur.2022.120442.
31. Mazinai, A., Zare, K., Moradi, O., Attar, H. (2022). Sulfonated calixarene modified poly(methyl methacrylate) nanoparticles: A promising adsorbent for removal of vanadium ions from aqueous media. *Chemosphere, 299*. DOI 10.1016/j.chemosphere.2022.134459.
32. Abdollahi, B., Salari, D., Zarei, M. (2022). Synthesis and characterization of magnetic Fe_3O_4@SiO_2-MIL-53(Fe) metal-organic framework and its application for efficient removal of arsenate from surface and ground water. *Journal of Environmental Chemical Engineering, 10, 107144*. DOI 10.1016/j.jece.2022.107144.
33. Abdollahi, B., Zarei, M., Salari, D. (2022). Synthesis, characterization, and application of diethylenetriamine functionalized MIL-53(Fe) metal-organic framework for efficient As(V) removal from surface and groundwater. *Journal of Solid State Chemistry, 299,* 123132. DOI 10.1016/j.jssc.2022.123132.